

December 11, 2012

The 2012 Moe/Thorpdale earthquake: Preliminary investigation

Dan Sandiford, Gary Gibson, Tim Rawling

School of Earth Sciences, University of Melbourne,

Abstract

The Strzelecki and Hoddle Ranges are fault-bounded hills in Gippsland Victoria, one of the most seismically active regions of the Australian Continent. The polygonal forms and loose symmetry of the two blocks suggests that past deformation has been partitioned on at least two sets of throughgoing structures. The nature of these structures at depth and their connection with current seismicity is not fully understood. The M_L 5.4 2012 Moe/Thorpdale earthquake was the largest Victorian event in thirty years (cf. 1982 M_L 5.4 near Mt. Sarah). The ongoing aftershock sequence comprises nearly 500 recorded events. This sequence provides the best opportunity so far to delineate active faults at depth beneath the Strzelecki Ranges. Here we present preliminary findings from the Moe/Thorpdale aftershock study. We are able to provide some provisional constraints on fault activity including focal mechanism solutions for the most significant groups of events in the aftershock sequence. The main aftershock (M_L 4.4) is seen to have occurred

Email address: sandd@student.unimelb.edu.au ()

shortly after a significant change in the recorded seismicity, with hypocentres becoming shallower and moving to the north. We interpret this change as the commencement of activity on one or more of the secondary structures in the Strzelecki fault network.

Keywords: Seismicity, Victoria, Neotectonics, Aftershocks, Gippsland

Introduction

Aftershocks of the M_L 5.4 Moe/Thorpdale earthquake that occurred at 10:53 UTC on the 19/06/12, were recorded by the University of Melbourne, Geoscience Australia, and the Environmental Systems & Services Seismology Research Centre. This was the the first deployment of the University of Melbourne aftershock instruments, acquired through the Australian Geophysical Observing System (AGOS). The combined study meant that up to 10 seismometer/accelerometer pairs were recording within 40 km of the epicentres, with many more stations outside this radius.

Seismicity of Gippsland

The majority of earthquakes recorded within the Australian continental interior are compressional in nature which supports stress models of the Indo-Australian plate based on heterogeneous plate boundary forces (*Coblentz et al.*, 1998). Much of the topography in the East Victorian Highlands (comprising the Victorian Alps and the hilly regions of Gippsland) is associated with mid to late Cenozoic block faulting (*Brown and Gibson*, 2004). Such faults are generally considered to be reactivated basement structures (*Morand*

et al., 2005). At least two sets of structures seem to be required to give the Strzelecki and Hoddle Ranges their distinctive polygonal forms. Geologically determined uplift rates on the order of ≈ 100 *m/ma* (0.1 *mm/a*) have been calculated for Gippsland (*Clark et al.*, 2011). Attempts to estimate seismic strain in Gippsland from *b*-value determinations have yielded values almost an order of magnitude higher than the geological constraints imply. The over-representation of M 4+ events in the catalogue is thought to be the cause of this discrepancy (*Sandiford et al.*, 2003).

From August 2000 to September 2001 a dense network of seismographs was operated in Gippsland, resulting in studies such as *Brown et al.* (2001). This period contained a significant earthquake by Australian standards, the M_L 4.9 Boolara South event. The earthquakes took place in near the Tarwin Graben, halfway between the bounding Yarragon and Yarram faults, leading to an ambiguity in the determination (if any) of a potential causative fault *Brown et al.* (2001). More recently the M_L 4+ Korumburra earthquakes of 2009 - 2011 are a possible instance of accelerated moment release (*Ben-Zion and Lyakhovskiy*, 2002) and may have taken place on the same fault as the 2012 events.

Figure 1 shows that historical seismicity is distinctly concentrated around the Strzelecki and Hoddle Ranges, intersecting the 2012 events.

General aftershock pattern

A subset of aftershocks (180) are shown in Figure 2. These events are ones for which a very clear polarity was shown at on the University of Melbourne

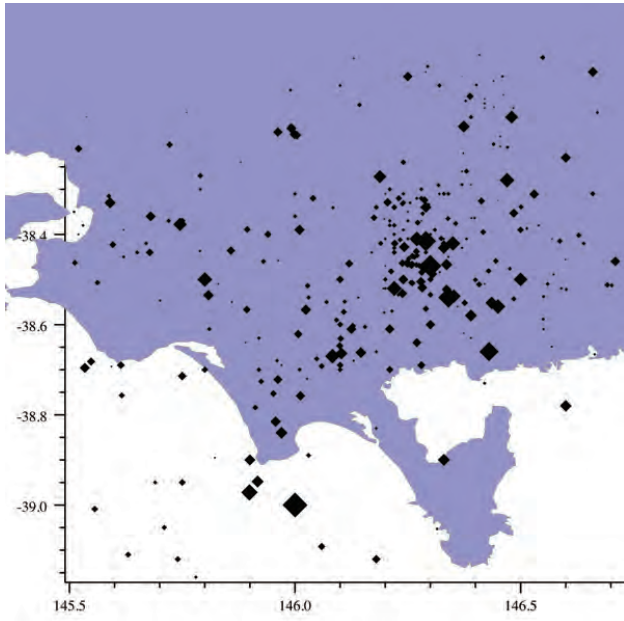


Figure 1: Historical seismicity of Gippsland, from the Geoscience Australia catalogue.

seismograph station LILL. It was observed that polarities at LILL fluctuated while those at nearby NARR (5 km) rarely did. Differentiating the events in this simple way reveal some of the key patterns in the aftershock sequence.

Figure 2 is sequential plot rather than a time series and as such it holds only broad information on the temporal distribution of aftershock events. We used the plot as a starting point to understand both the spatial and temporal distribution of events. The most obvious feature of Figure 2 is the change between what are termed the ‘early’ phase and ‘late’ phase aftershock events. These two main phases of activity are separated by a step-like change in S minus P arrival times at LILL.

Figure 5 shows composite focal mechanisms derived from early phase events

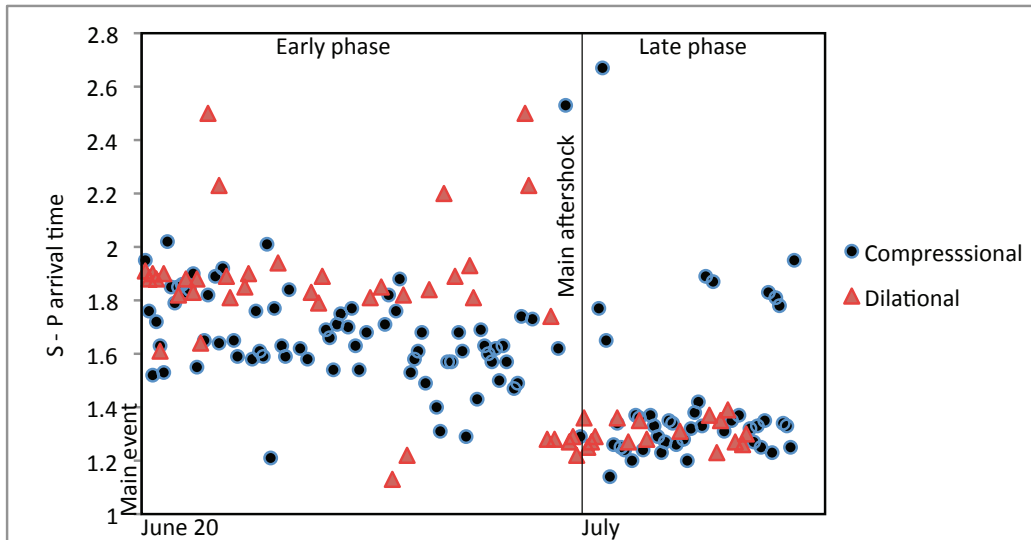


Figure 2: A subset of the aftershocks. Events are plotted sequentially so the time axis is not scaled linearly.

across the aftershock study network. The dominant polarity pattern for each subset of earthquakes is also represented on a Digital Elevation Model of the Stzrelecki Ranges. Events were separated firstly on the basis of polarity (up: ‘c’, down: ‘d’, or small/ambiguous: ‘e’) at LILL and secondly on a spatial basis where this resulted in a significant decrease in focal mechanism solution (FMS) misfit. The aim was to create composite focal mechanisms that represented true event clustering without subdividing the catalogue too heavily.

Early Phase

Figure 2 shows that there is slight S minus P time offset for early ‘c’ and ‘d’ events at LILL. The depth range of these events is 10–16 km. We suggest

that activity on at least two separate faults is required to reconcile the first motion pattern across the network and that the polarity at LILL is in most cases a telltale for which of the faults slip occurred on. The requirement that two faults are active can be reasonably inferred by considering the oscillation of polarities at the stations LILL, NARR & MOE4 (forming a roughly SE—NW line across the epicentral region). Polarities at NARR are always positive while at LILL a large fraction, 20–30% of events, are negative. It was observed that in the majority of cases the polarity at MOE4 changes when LILL does so as they usually retain opposite polarity. In other words, polarity changes frequently occur simultaneously on opposite sides of NARR. If the events were situated on different parts of the same fault one of the nodal planes (indeed the fault plane) would be expected to remain at a similar orientation and therefore intersect the surface through a semi regular axis. The fact that the three stations are near inline and that the nodal planes shift on either side of the central station seems to require that the early aftershock events are the product of activity on two separate faults.

A cross section through the early ‘c’ events shows a dip sense that is up to the SE, down to the NW. At this stage there are not enough well-located events in this subset to determine whether this is a real trend or an artifact. A best fit through these events probably describes a plane that is too shallow to represent the larger fault (20 degrees). On the other hand the FMS resolves a steeper plane (possibly too steep) of about 50 degrees. There are a number of faults to the SE of the epicenters that match the FMS strike. This is not the case if the FMS is interpreted in an inverse sense (a SE dipping plane) unless we postulate an anomalously steep dip (70 degrees) on the Yarragon

Fault. At this stage the Tarwin Fault seems like the most likely candidate for a NW dipping fault.

The early phase ‘d’ events at LILL yield a FMS with a very well constrained vertically dipping plane striking at 251 degrees. These events could be interpreted as either a horizontal slip vector on a moderately steep (50 degrees) SW dipping plane, or as a slip on a near vertical plane with a non-horizontal slip vector. There are mapped faults corresponding to either of these solutions. At this stage there are not enough well located events as to favour one or other. The theoretical constraint that one of principal stress axes is near vertical does not help to discriminate given that both solutions would require a similar rotation away from this idealised stress state. First motion on the East and North channels favour the former.

Late Phase

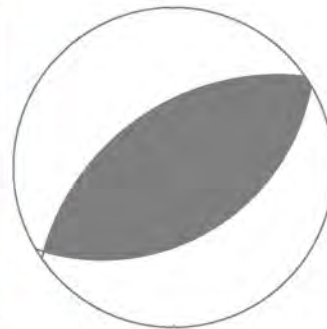
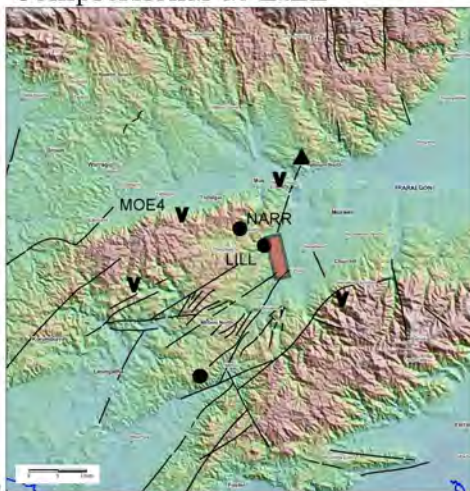
The late phase events are shown in Figure 4 . The epicentral region is seen to have moved to the N, while the average depth of events shallowed to 7–10 km. Again, the events were subdivided on the basis of polarity at LILL which remained oscillatory. The polarity on the vertical channel at NARR remained positive in almost all events. The FMS for the late phase events are all varieties of dip-slip faulting with a compressional quadrant that encompasses NARR, and variably encompasses other stations along a NE—SW axis including LILL, MOE4, MOE6 and HOLS. Between the early phase and late phase events a new station called CREM about 6 km to the SE of LILL was installed. In the late phase events CREM polarities are always

negative, providing a fixed constraint that one of the nodal planes lies to the NW of the station. On the basis of polarity late phase events are not forced to derive from more than one fault (as in the early phase events). There is no observed S minus P time difference for late phase ‘c’ or ‘d’ events. At this stage the FMS for the two subsets of late events (Figure 4) are reasonably similar. Faults that would fit the FMS are either a NNE striking, WNW dipping fault that intersects the surface to the east of the epicenters (The Haunted Hill fault, Morwell Fault or Balook fault are candidates.) or a NE striking SW dipping fault intersecting the surface to the north of the epicenters. In the later case, a mapped fault does not present itself unless we postulate an anomalously steep dip (70 degrees) on the Yarragon Fault. There is no evidence so far that the late events take place on separate faults.

Conclusions

The preliminary aftershock study of the 2012 Moe/Thorpdale earthquake has identified two major phases of activity and provided some provisional constraints on the faults that generated the majority of events. One of the most interesting aspects of the aftershock sequence is the mode change that occurs shortly before the main aftershock. We have suggested that such a change is compatible with commencing of activity on a secondary structure set striking NNE, such as the Haunted Hill Fault. If we are able to confirm this pattern we will gain an insight into the way that deformation is partitioned on primary and secondary structures in the Strzelecki Ranges. The observation of a mode change as a precursor to the main aftershock may serve as an example for assessing hazard in other aftershock sequences.

Compressional at LILL

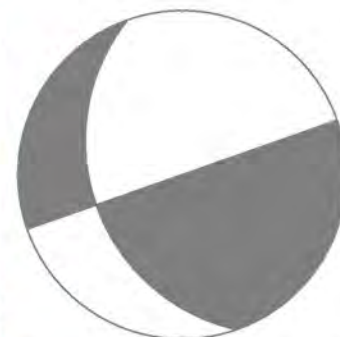
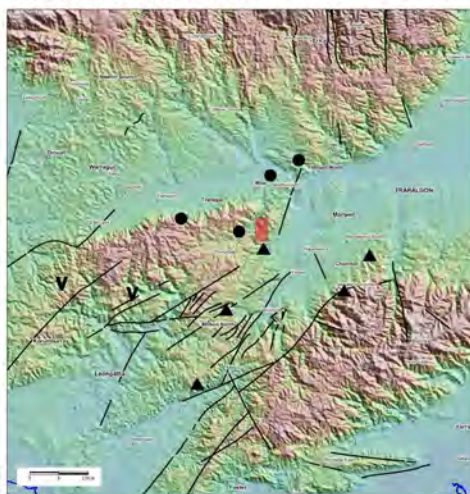


6 events, 46 polarities, 6 misfits
[235, 49, 87]

a

• = compressional ▲ = dilational
V = variable E = emergent
■ = epicentre region

Dilational at LILL

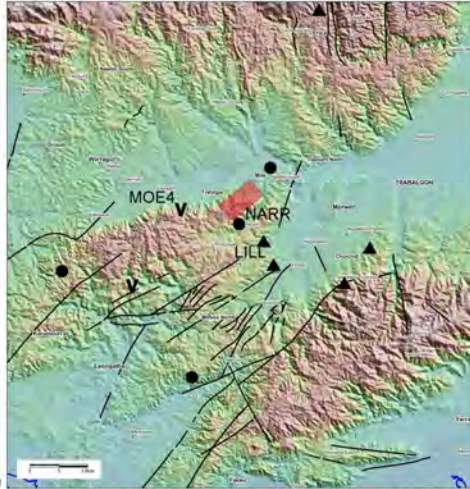


8 events, 47 polarities, 3 misfits
[251, 90, 58]

b

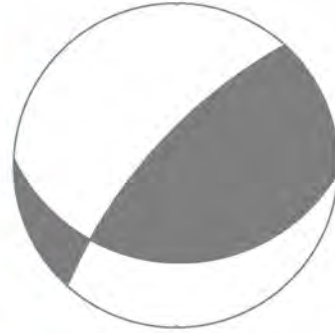
Figure 3: Early events separated according to polarity at LILL.

Dilational at LILL



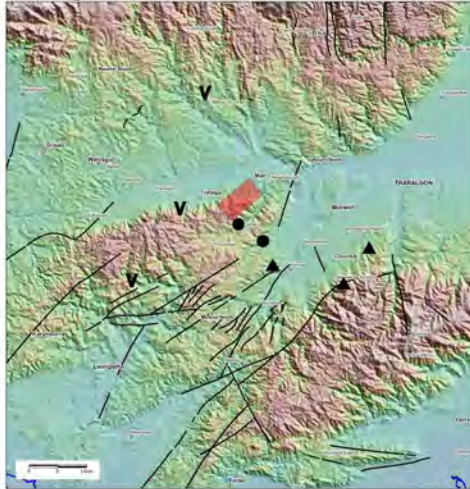
a

● = compressional ▲ = dilational
 V = variable E = emergent
 ■ = epicentre region

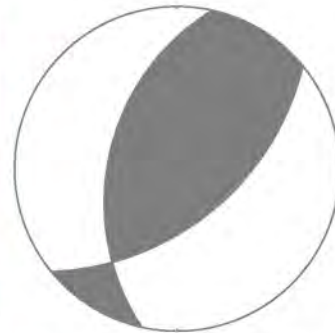


6 events, 35 polarities, 3 misfits

Compressional at LILL



b



6 events, 27 polarities, 3 misfits

Figure 4: Late events separated according to polarity at LILL

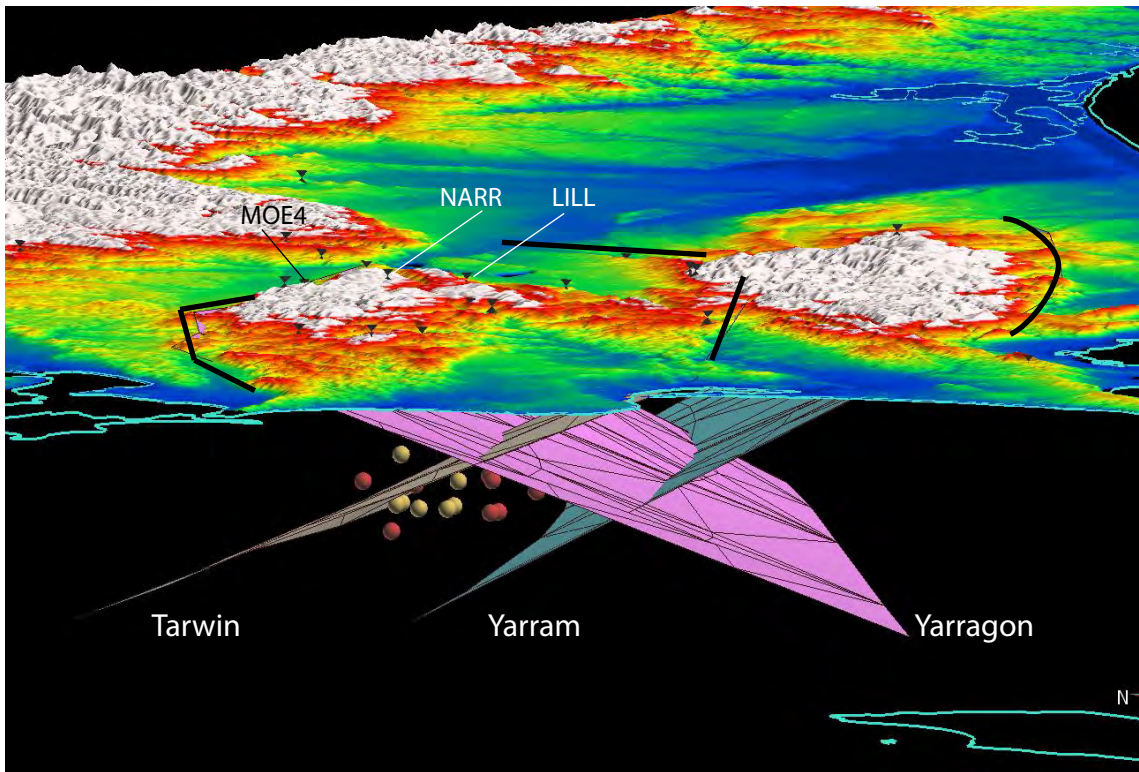


Figure 5: Main reverse faults, inferred from geomorphic expression, as well as a subset of early events. The Tarwin fault dipping at theoretically-optimal 30 degrees intersects the events well. View is to the west.

Acknowledgements

The aftershock study was a cooperative effort carried out by the University of Melbourne through the A.G.O.S Subsurface Observatory, and Geoscience Australia. The Environmental Systems and Services Seismology Research Centre assisted throughout with data analysis, data sharing, valuable advice. Seismic data processing was carried out on ES&S EqSuite software as well as SEISAN. DEMs are from Victorian Department of Primary Industries. The ongoing help of many people in the Strzelecki region who let us install instruments on their properties is gratefully acknowledged.

References

- Ben-Zion, Y., and V. Lyakhovsky, Accelerated seismic release and related aspects of seismicity patterns on earthquake faults, *Earthquake Processes: Physical Modelling, Numerical Simulation and Data Analysis Part II*, pp. 2385–2412, 2002.
- Brown, A., and G. Gibson, A multi-tiered earthquake hazard model for australia, *Tectonophysics*, 390, 25–43, 2004.
- Brown, A., T. Allen, and G. Gibson, Seismicity and earthquake hazard in gippsland, victoria, *Proceeding of the Australian Earthquake Engineering Society*, pp. 1–538, 2001.
- Clark, D., A. McPherson, and C. Collins, Australias seismogenic neotectonic record: a case for heterogeneous intraplate deformation, *Geoscience Australia, Canberra*, 2011.

- Coblentz, D., S. Zhou, R. Hillis, R. Richardson, and M. Sandiford, Topography, boundary forces, and the indo-australian intraplate stress field, *Journal of Geophysical Research*, *103*, 919–931, 1998.
- Morand, V. J., B. A. Simons, D. Taylor, C. A., S. Maher, , K. Wohlt, and A. M. Radojkovic, Bogong 1:100 000 map area geological report, *Geoscience Survey of Victoria Report 125*, 2005.
- Sandiford, M., M. Leonard, and D. Coblentz, Geological constraints on active seismicity in southeast australia, *Earthquake Risk Mitigation*, pp. 1–10, 2003.